

SHORT REPORT

Open Access



Severe COVID-19-associated variants linked to chemokine receptor gene control in monocytes and macrophages

Bernard S. Stikker¹, Grégoire Stik^{2,3†}, Antoinette F. van Ouwerkerk^{4†}, Lianne Trap¹, Salvatore Spicuglia⁴, Rudi W. Hendriks¹ and Ralph Stadhouders^{1,5*} 

*Correspondence: r.stadhouders@erasmusmc.nl
†Grégoire Stik and Antoinette F. van Ouwerkerk contributed equally to this work.
¹ Department of Pulmonary Medicine, Erasmus MC, University Medical Center Rotterdam, Rotterdam, The Netherlands
Full list of author information is available at the end of the article

Abstract

Genome-wide association studies have identified 3p21.31 as the main risk locus for severe COVID-19, although underlying mechanisms remain elusive. We perform an epigenomic dissection of 3p21.31, identifying a CTCF-dependent tissue-specific 3D regulatory chromatin hub that controls the activity of several chemokine receptor genes. Risk SNPs colocalize with regulatory elements and are linked to increased expression of *CCR1*, *CCR2* and *CCR5* in monocytes and macrophages. As excessive organ infiltration of inflammatory monocytes and macrophages is a hallmark of severe COVID-19, our findings provide a rationale for the genetic association of 3p21.31 variants with elevated risk of hospitalization upon SARS-CoV-2 infection.

Keywords: SARS-CoV-2, COVID-19, 3p21.31, GWAS, Monocyte, Macrophage, Chemokine receptor, 3D genome organization, CTCF, Gene regulation

Background

Coronavirus disease 2019 (COVID-19) is a potentially life-threatening respiratory disorder caused by the severe acute respiratory syndrome coronavirus 2 (SARS-CoV-2) [1]. Clinical manifestations of SARS-CoV-2 infection range from no or mild symptoms to respiratory failure. Life-threatening disease is often associated with an excessive inflammatory response to SARS-CoV-2, involving elevated systemic cytokine levels and profound organ infiltration by monocytes and macrophages [2, 3]. Besides clinical characteristics such as age and various comorbidities [4], genetic differences play a role in predisposing individuals to progress towards severe disease [5, 6]. In genome-wide association studies (GWASs), the 3p21.31 locus was strongly associated with increased risks of morbidity and mortality - in particular for younger (≤ 60 years) individuals [7]. However, it is currently still largely unclear how variants and genes in this locus affect the immune response against SARS-CoV-2 and COVID-19 disease pathophysiology.



© The Author(s) 2022. **Open Access** This article is licensed under a Creative Commons Attribution 4.0 International License, which permits use, sharing, adaptation, distribution and reproduction in any medium or format, as long as you give appropriate credit to the original author(s) and the source, provide a link to the Creative Commons licence, and indicate if changes were made. The images or other third party material in this article are included in the article's Creative Commons licence, unless indicated otherwise in a credit line to the material. If material is not included in the article's Creative Commons licence and your intended use is not permitted by statutory regulation or exceeds the permitted use, you will need to obtain permission directly from the copyright holder. To view a copy of this licence, visit <http://creativecommons.org/licenses/by/4.0/>. The Creative Commons Public Domain Dedication waiver (<http://creativecommons.org/publicdomain/zero/1.0/>) applies to the data made available in this article, unless otherwise stated in a credit line to the data.

Results and discussion

COVID-19 GWAS meta-analyses (release 4 by the COVID-19 Host Genetics Initiative [8]) confirmed the strong association between the 3p21.31 locus and COVID-19, both when comparing hospitalized COVID-19 patients with healthy control subjects (Additional file 1: Fig.S1a) or with non-hospitalized patients (Additional file 1: Fig. S1b), indicating a stronger link with more severe disease. We focused on the former comparison (8638 hospitalized COVID-19 patients vs. 1,736,547 control subjects) to maximize the number of associated SNPs available for downstream analysis. Regional association plots generated using the Functional Mapping and Annotation (FUMA) platform [9] revealed a region of 743 kb with 21 independent significant ($P < 5e-8$) GWAS SNPs and hundreds of variants in high linkage disequilibrium (LD; $r^2 > 0.8$) (Fig. 1a). Approximately 96% of these SNPs fall in non-coding regions adjacent to 12 known protein-coding genes (Fig. 1a).

Common disease-associated genetic variants predominantly localize to regulatory DNA elements [11]. To identify disease-relevant candidate genes and gene regulatory regions at 3p21.31, we integrated GWAS findings with publicly available data from large-scale transcriptomics and epigenome profiling studies. Special emphasis was placed on immune cells, as detrimental hyperinflammation is characteristic of severe COVID-19 [2, 3]. Analysis of histone 3 lysine 27 acetylation (H3K27Ac) profiles from ENCODE [12] and BLUEPRINT [13] databases revealed cell type-specific active gene regulatory elements (GREs) at 3p21.31, with particularly strong activity seen in monocytes, monocyte-derived macrophages and neutrophils (Fig. 1b, c, Additional file 1: Fig.S2). The largest fraction of disease-associated SNPs overlapped with monocyte H3K27Ac⁺ GREs, which were concentrated in three active chromatin regions (ACRs) near the *CCR1*, *CCR2*, *CCR3* and *CCR5* genes (Fig. 1b, c). *CCR1* and *CCR2* are critical mediators of monocyte/macrophage polarization and tissue infiltration [14], which are pathogenic hallmarks of severe COVID-19 [2, 3]. The three ACRs also showed substantial chromatin accessibility (as measured by DNase-Seq) in monocytes (Additional file 1: Fig.S2). Gene expression analysis using data from 6 transcriptome repositories (see the “Methods” section) confirmed strong transcriptional activity of the 3' *CCR* genes in tissues containing haematopoietic cells (e.g. whole blood, spleen), with especially *CCR1* and *CCR2* being highly expressed in classical monocytes, macrophages and neutrophils (Fig. 1d, Additional file 1: Figs. S2-S3). Of note, several other immune cell subsets, including T cell and dendritic cell subsets, also expressed specific *CCR* genes (Fig. 1d, Additional file 1: Figs. S2-S3). Chromatin interaction profiles from primary immune cells (measured by promoter-capture Hi-C [15]) revealed extensive monocyte/macrophage-specific chromatin interactions between the three ACRs, as exemplified by *CCR1* promoter interaction profiles in monocyte-derived macrophages and T cells (Fig. 1e, Additional file 1: Fig. S4a-b). In all immune cells profiled by Javierre et al. [15], no significant interactions were detected between 3p21.31 gene promoters and the lead SNP region or the most distal SNPs in *LIMD1* (Additional file 1: Fig.S4c), although HindIII-based promoter-capture Hi-C has limited resolution very close (<20 kb) to viewpoints.

Together, this analysis reveals the strong transcriptional activity of a *CCR* gene cluster within the 3p21.31 COVID-19 risk locus in immune cells, especially in monocytes and macrophages. Activity is centred around *CCR1* and its genomic surroundings, which

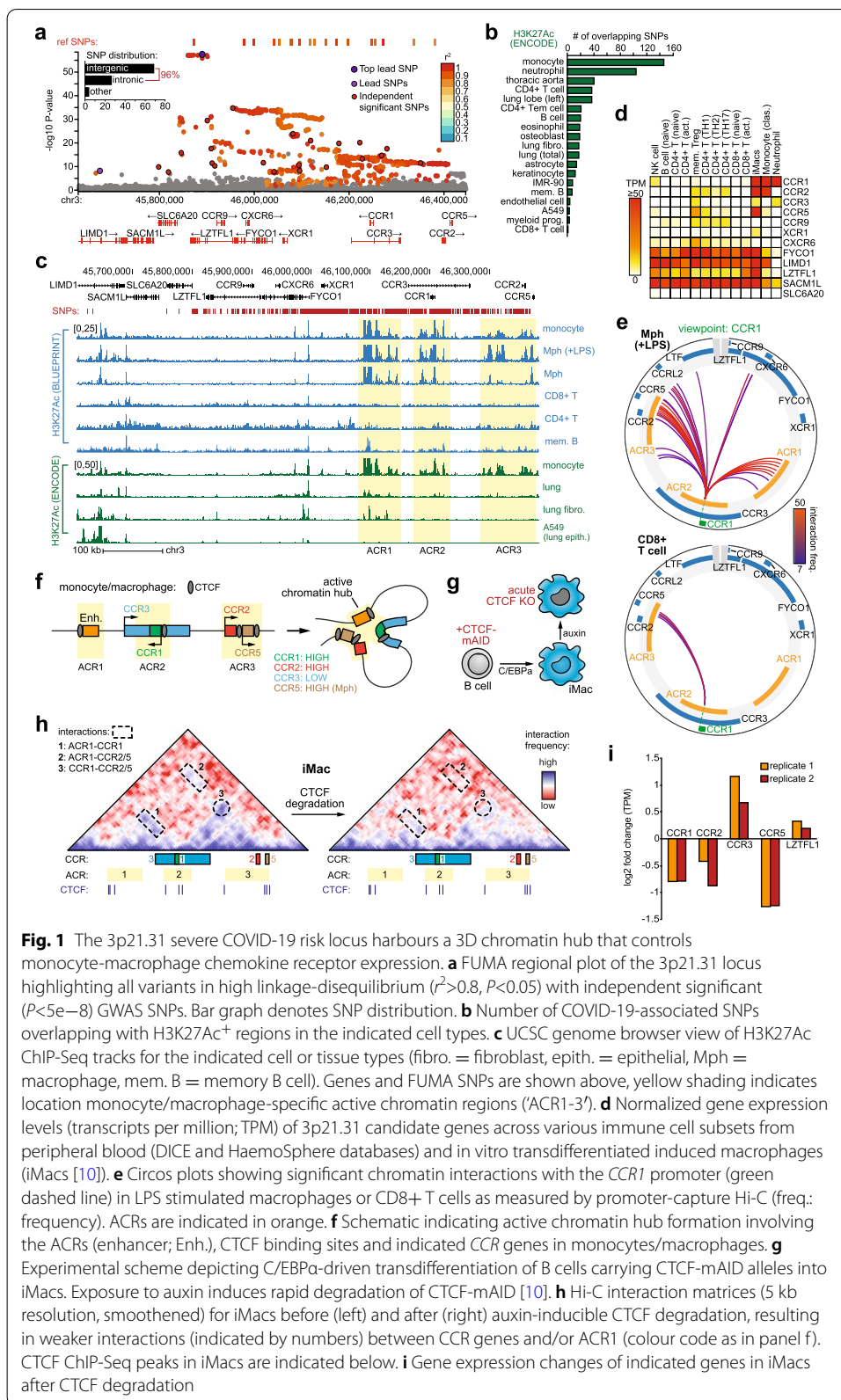
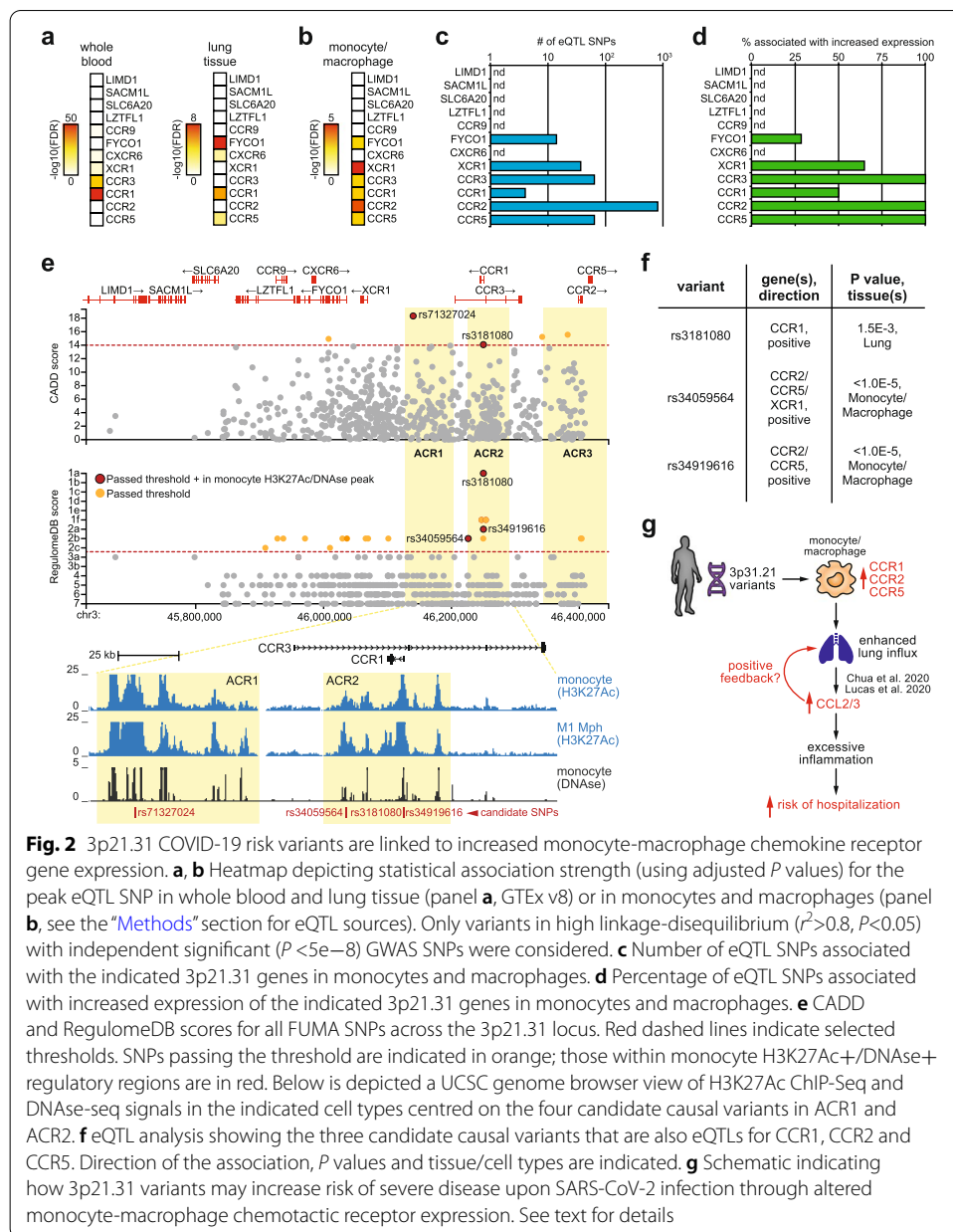


Fig. 1 The 3p21.31 severe COVID-19 risk locus harbours a 3D chromatin hub that controls monocyte-macrophage chemokine receptor expression. **a** FUMA regional plot of the 3p21.31 locus highlighting all variants in high linkage-disequilibrium ($r^2 > 0.8$, $P < 0.05$) with independent significant ($P < 5e-8$) GWAS SNPs. Bar graph denotes SNP distribution. **b** Number of COVID-19-associated SNPs overlapping with H3K27Ac⁺ regions in the indicated cell types. **c** UCSC genome browser view of H3K27Ac ChIP-Seq tracks for the indicated cell or tissue types (fibro. = fibroblast, epith. = epithelial, Mph = macrophage, mem. B = memory B cell). Genes and FUMA SNPs are shown above, yellow shading indicates location monocyte/macrophage-specific active chromatin regions (‘ACR1-3’). **d** Normalized gene expression levels (transcripts per million; TPM) of 3p21.31 candidate genes across various immune cell subsets from peripheral blood (DICE and HaemoSphere databases) and in vitro transdifferentiated induced macrophages (iMacs [10]). **e** Circos plots showing significant chromatin interactions with the *CCR1* promoter (green dashed line) in LPS stimulated macrophages or CD8+ T cells as measured by promoter-capture Hi-C (freq.: frequency). ACRs are indicated in orange. **f** Schematic indicating active chromatin hub formation involving the ACRs (enhancer; Enh.), CTCF binding sites and indicated *CCR* genes in monocytes/macrophages. **g** Experimental scheme depicting *C/EBPα*-driven transdifferentiation of B cells carrying CTCF-mAID alleles into iMacs. Exposure to auxin induces rapid degradation of CTCF-mAID [10]. **h** Hi-C interaction matrices (5 kb resolution, smoothed) for iMacs before (left) and after (right) auxin-inducible CTCF degradation, resulting in weaker interactions (indicated by numbers) between *CCR* genes and/or *ACR1* (colour code as in panel f). CTCF ChIP-Seq peaks in iMacs are indicated below. **i** Gene expression changes of indicated genes in iMacs after CTCF degradation

are organized in a 3D chromatin hub involving the other active *CCR* genes (i.e. *CCR2*, *CCR5*) and putative enhancer elements (Fig. 1f)—a chromatin conformation often used for complex tissue-specific gene regulation [16]. To further substantiate the relevance of local 3D chromatin organization for 3p21.31 *CCR* gene regulation in myeloid cells, we used epigenomics data from the BLaER induced macrophage (iMac) cell line system [10]. The iMacs, which morphologically and functionally closely resemble macrophages [17], showed highly comparable H3K27Ac enrichment at the 3p21.31 ACRs and expressed high levels of *CCR1*, *CCR2* and *CCR5* (Additional file 1: Fig.S5a-b). High-resolution in-situ Hi-C data [10] of iMacs revealed that the 3p21.31 COVID-19-associated genomic block resides in the nuclear A compartment (Additional file 1: Fig.S5c), a chromosomal compartment located in the nuclear interior that groups together transcriptionally active chromatin [18]. Zooming in, we observed that most of the 3p21.31 risk variants and all associated chemokine receptor genes localize to a single topologically associating domain (TAD) (Additional file 1: Fig.S5d), representing an insulated genomic neighbourhood that promotes establishing interactions between genes and regulatory elements inside the TAD [18]. Interestingly, ACR1 and ACR3 were flanked by strong binding sites for the genome architectural CCCTC-binding factor CTCF [19] in iMacs and primary monocytes (Additional file 1: Fig.S5a). Together with the presence of additional CTCF binding sites within all three ACRs, including the *CCR1* promoter region (Additional file 1: Fig.S5a), these data suggest that CTCF organizes local 3D active chromatin hub formation to insulate the *CCR3-CCR1-CCR2-CCR5* gene cluster for transcriptional regulation. To test this hypothesis, we leveraged our recently developed iMac line expressing CTCF fused to an auxin-inducible degron (mAID), which allows for rapid degradation of CTCF and disruption of 3D genome architecture (Fig. 1g) [10]. Detailed Hi-C analysis confirmed the presence of strong interactions between the ACRs and 3' *CCR* genes in iMacs, which were disrupted upon CTCF depletion (Fig. 1h). Importantly, chromatin hub decommissioning specifically reduced *CCR1*, *CCR2* and *CCR5* expression (Fig. 1i), revealing that CTCF-mediated 3D chromatin interactions are critical for regulating 3p21.31 *CCR* gene activity in macrophages. Of note, expression of the *CCRL2* gene just downstream of *CCR5*—encoding an atypical chemokine receptor involved in macrophage polarization [20]—was only marginally affected by CTCF depletion (\log_2 fold change of 0.23).

We next sought to directly link COVID-19-associated genetic variants to altered 3' *CCR* gene expression in myeloid immune cells. To this end, we used FUMA to systematically analyze previously reported expression quantitative trait loci (eQTLs) overlapping with the 958 COVID-19-associated ($P < 5e-8$) SNPs. As eQTL sources, we focused on disease-relevant tissues rich in monocytes/macrophages (i.e. whole blood and lung tissue) and studies using purified monocytes or in vitro differentiated macrophages (see the “Methods” section). The 3' 3p21.31 *CCR* genes showed highly significant eQTL associations (FDR < 0.05) with COVID-19-associated variants, especially in monocytes and macrophages (Fig. 2a, b). Multiple risk SNPs were identified as eQTLs for *CCR1*, *CCR2*, *CCR3* and *CCR5* in monocytes/macrophages, with the majority correlating with increased gene expression (Fig. 2c, d). No eQTL associations were detected for *CCRL2*. To further prioritize variants with potential biological significance we used RegulomeDB [21] and CADD [22] SNP annotations.



Stringent filters for both scores were combined with localization within a putative monocyte regulatory region (H3K27Ac⁺ and DNase⁺), yielding four unique candidate causal SNPs of which three were associated with increased *CCR1*, *CCR2* and/or *CCR5* expression (Fig. 2e, f). These variants did not engage in significant interactions with sequences far outside the susceptibility region, e.g. beyond the *CCR* gene cluster (Additional file 1: Fig.S6). Candidate causal variants mostly clustered within *ACR2* and altered putative transcription factor binding motifs, readily providing testable hypotheses for future investigations (Additional file 1: Fig.S7). For example, two SNPs within the *CCR1* promoter affected binding motifs of known regulators of the macrophage inflammatory expression programme (Additional file 1: Fig.S7a-b). Variant

rs3181080 optimizes a composite Interferon Regulatory Factor (IRF)-Activator Protein 1 (AP1) motif, which is used for cooperative binding of IRF and AP1 family transcription factors that promote monocyte/macrophage activation [23]. In line with *CCR1* activation by IRF/AP1 factors, binding of AP1 proteins and IRF4 to rs3181080 was detected in *CCR1*-expressing GM12878 lymphoblastoid cells (Additional File 1: Fig.S7c). Previous experiments in mouse macrophages [24] confirmed IRF binding to the *Ccr1* promoter (Additional file 1: Fig.S7d). The second *CCR1* promoter variant, rs34919616, disrupts a critical nucleotide in a motif for BCL6 (Additional file 1: Fig. S7a-b), a suppressor of inflammatory gene expression in macrophages [25].

Taken together, these data show that the COVID-19-associated 3p21.31 locus harbours a CTCF-dependent tissue-specific 3D chromatin hub that controls chemotactic receptor expression in monocytes and macrophages. Several 3p21.31 variants localize to gene regulatory elements within this chromatin hub and are associated with elevated *CCR1*, *CCR2*, *CCR3* and *CCR5* expression, which is further supported by a recent transcriptome-wide association study in lung tissue [6]. Mechanistically, these risk variants may modulate transcription factor binding at *CCR* gene regulatory elements. *CCR1*, *CCR2* and *CCR5* upregulation could enhance lung infiltration by monocytes and macrophages upon viral infection [14], contributing to the rapid and deleterious hyperinflammation observed in COVID-19 patients suffering from severe disease [2, 3] (Fig. 2g). In support of this notion, single cell transcriptomics revealed increased levels of *CCR1* and *CCR5* as well as their ligands *CCL2/CCL3* specifically in pulmonary macrophages from critical COVID-19 patients [26, 27]. Additionally, *CCL2* plasma levels showed the highest predictive value for mortality in a COVID-19 patient cohort [28]. These findings are in line with excessive pulmonary influx of monocytes and subsequent differentiation into inflammatory tissue macrophages as a hallmark of severe COVID-19 (Fig. 2g) [26].

Our analysis has several limitations. Although we provide compelling evidence for monocyte-macrophage 3' *CCR* gene activity linked to 3p21.31 risk variants, several other immune cell types involved in antiviral immunity also express some of these chemokine receptors (e.g. *CCR1* on neutrophils, *CCR5* on T cell subsets) and may therefore also be affected by the genetic variants. Moreover, although our analysis detected fewer non-coding regulatory activity in the 5' part of the 3p21.31 COVID-19-associated genomic block, this region harbours the lead SNP and several actively transcribed genes with more housekeeping-like expression patterns, which may also be relevant for COVID-19 pathophysiology. Indeed, Downes et al. recently reported that a variant in high LD with the lead SNPs affects an enhancer of *LZTFL1* in non-immune cells, with potential implications for anti-viral responses [29]. Although variants in the lead SNP region were also reported as eQTLs for *CCR2* and *CCR5* in monocytes and macrophages, this likely reflects the high LD ($r^2 > 0.8$) of these variants with the 3' *CCR* SNPs (Fig. 1a). In support of this notion, genetic deletion of a 68kb region around the lead SNP in a myeloid cell line did not affect 3' 3p21.31 *CCR* gene expression [30] and Downes et al. found no evidence of these SNPs disrupting gene regulatory mechanisms in immune cells [29]. Another study integrating loss-of-function experiments in an airway epithelial carcinoma cell line with eQTL data implicated *SLC6A20* and *CXCR6* in COVID-19 pathophysiology [31], whereas deleting the lead SNP region resulted in reduced *CCR9* and *SLC6A20* expression in leukemic T cells [30]. Future investigations including additional (non-immune)

cell types are required to further elucidate the candidate causal genes operating in different cell types and/or under different microenvironmental circumstances.

Conclusions

Our data support a scenario in which common genetic variants increase susceptibility to develop severe COVID-19 by affecting gene regulatory control of monocyte-macrophage chemotactic receptor expression. As a consequence, elevated migratory capacity of monocytes and macrophages could contribute to aggravated inflammatory responses and more severe disease. These data add to our understanding of the genetic basis of COVID-19 disease heterogeneity and support exploring therapeutic targeting of monocyte-macrophage 3p21.31 CCR activity in hospitalized COVID-19 patients.

Methods

GWAS data retrieval

Version 4 COVID-19 GWAS meta-analysis data was retrieved from The COVID-19 Host Genetics Initiative at <https://www.covid19hg.org/>. GWAS data (GRCh37/hg38 genome build) was obtained from two studies: B1_ALL (hospitalized COVID-19 vs. non-hospitalized COVID-19; 2430 cases versus 8478 controls) and B2_ALL (hospitalized COVID-19 vs. population; 8638 cases versus 1,736,547 controls). GWAS summary statistics files were used to generate input files for FUMA using standard data frame processing functions in Rstudio v.1.3.

Identification of a high LD block of COVID-19 associated SNPs

FUMA [9] was performed for both B1_ALL and B2_ALL GWASs (version 4 summary statistics downloaded from <https://www.covid19hg.org/>) using default settings, with exception of the r^2 (LD) used to define independent significant SNPs, which was set to ≥ 0.8 . Manhattan and regional plots were generated by FUMA's SNP2GENE function. Significant FUMA SNPs were converted to GRCh38/hg38 using UCSC LiftOver (<https://genome.ucsc.edu/cgi-bin/hgLiftOver>) to allow aligning variants to the epigenomic profiles.

ChIP-Seq, DNase-Seq and (promoter-capture) Hi-C data analysis

ChIP-Seq and DNase-Seq epigenomic data used were retrieved from public ENCODE [12] and BLUEPRINT [13] databases. Data were visualized in the UCSC Genome Browser (<https://genome.ucsc.edu>). The *intersect* function of BEDTools [32] was used to determine the number of FUMA SNPs overlapping with H3K27Ac⁺ regions in the indicated cell types. Peak calling files for each H3K27Ac dataset were directly obtained from the ENCODE website (<https://www.encodeproject.org/>). Circos plots visualizing promoter-capture HiC data from the BLUEPRINT consortium [15] were generated using <https://www.chicp.org/chicp/>, with a threshold normalized interaction value of 7. ChIP-Seq and in-situ Hi-C data from in vitro transdifferentiated macrophages (induced macrophages or iMacs), both prior to and after auxin-inducible CTCF degradation, were obtained from GSE140528 and analysed as previously described [10].

Gene expression analysis

RNA-Seq profiles from a broad spectrum of selected relevant cell types were obtained from public ENCODE [12] and BLUEPRINT [13] databases and visualized in the UCSC Genome Browser. Expression value heatmaps from various collection of (immune) cell types were obtained from DICE [33] (<https://dice-database.org/>), GTEx v8 [34] (via FUMA's GENE2FUNCTION function), BioGPS [35] (<http://biogps.org/>), Haemosphere [36] (<https://www.haemosphere.org/>) and Monaco et al. [37] (GSE107011). Transcripts per million (TPM) values were visualized as averaged values using Morpheus (<https://software.broadinstitute.org/morpheus/>). RNA-Seq and TPM values for iMacs were obtained from GSE140528 and analysed as previously described [10].

Candidate causal variant filtering

The Combined Annotation Dependent Depletion (CADD [22]) and RegulomeDB [21] scores for all significantly associated SNPs were also obtained from FUMA. As thresholds to identify candidate causal variants, we used CADD scores >14 and RegulomeDB scores <3. SNPs were further filtered based on their combined overlap with H3K27Ac ChIP-Seq and DNase-seq peaks in monocytes (data obtained from ENCODE [12]). Transcription factor binding motifs were obtained using HOMER [38].

Expression quantitative trait locus (eQTL) analysis

eQTL analysis was performed using FUMA, focusing on tissues relevant for COVID-19 pathophysiology and enriched for monocytes/macrophages (i.e. whole blood and lung from GTEx v8 [34]) or studies using monocytes and/or *in vitro* differentiated macrophages [39–41]. Thresholds for statistical significance were set to FDR<0.05.

Supplementary Information

The online version contains supplementary material available at <https://doi.org/10.1186/s13059-022-02669-z>.

Additional file 1: Figure S1. Overview of genome-wide genetic associations with severe COVID-19. **Figure S2.** Transcriptional and epigenomic activity at 3p21.31 in selected cell types. **Figure S3.** Gene expression analysis of 3p21.31 candidate genes across various nonimmune and immune cells types. **Figure S4.** Regulatory chromatin interactions across the 3p21.31 COVID-19 risk locus. **Figure S5.** Epigenomic landscape and 3D genome folding at the 3p21.31 COVID-19 risk locus in iMacs. **Figure S6.** Chromatin interactions with prioritized 3p21.31 COVID-19 risk variants. **Figure S7.** 3p21.31 COVID-19 risk variants disrupt putative transcription factor binding sites.

Additional file 2: Table S1. Database accession numbers of individual datasets used and accompanying citations used throughout this study.

Additional file 3. Review history.

Acknowledgements

We thank staff of the Erasmus MC Pulmonary Medicine department for fruitful discussions. We are indebted to the COVID-19 Host Genetics Initiative for immediately making their GWAS analyses publically available, and to the genomics consortia that provide the scientific community with invaluable data.

Peer review information

Kevin Pang was the primary editor of this article and managed its editorial process and peer review in collaboration with the rest of the editorial team.

Review history

The review history is available as Additional file 3.

Authors' contributions

Study conception and design: B.S., R.W.H. and R.S.; data acquisition: B.S., G.S., A.F.v.O. and R.S.; analysis and interpretation of data: B.S., G.S., A.F.v.O., S.S., R.W.H. and R.S.; drafting of manuscript: B.S., R.W.H. and R.S.; critical revision: all authors. The authors read and approved the final manuscript.

Funding

B.S. and R.W.H. are supported by Dutch Lung Foundation grant 4.1.18.226. G.S. was supported by the 'Fundación Científica de la Asociación Española Contra el Cáncer'. R.S. is supported by an Erasmus MC Fellowship, a Dutch Lung Foundation Junior Investigator grant (4.2.19.041JO) and a VIDI grant (09150172010068) from the Dutch Research Council (NWO). A.F.v.O. was supported by a postdoctoral fellowship from the Foundation Recherche Médicale. S.S. was supported by an Agence National pour la Recherche" grant (ANR-18-CE12-0019).

Availability of data and materials

All datasets generated and/or analysed during the current study are available in the public repositories and/or using the persistent web links (also see [Methods](#) section): GWAS data was retrieved from <https://www.covid19hg.org/> (version 4, B1_ALL & B2_ALL); FUMA analysis (including eQTL analysis) was performed using <https://fuma.ctglab.nl/>; ChIP-Seq, DNase-Seq and RNA-Seq data used were retrieved from public ENCODE (<https://www.encodeproject.org/>), BLUEPRINT (<http://dcc.blueprint-epigenome.eu/#/home>), DICE (<https://dice-database.org/>), GTEx (<https://gtexportal.org/home/>), BioGPS (<http://biogps.org/>) and Haemosphere (<https://www.haemosphere.org/>) databases; epigenomics data was visualized in the UCSC Genome Browser (<https://genome.ucsc.edu/>); promoter-capture Hi-C data from the BLUEPRINT consortium was visualized using <https://www.chicp.org/chicp/>; iMac Hi-C and RNA-Seq data was obtained from GSE140528; heatmaps were generated using Morpheus (<https://software.broadinstitute.org/morpheus/>). Database accession numbers of individual datasets used and accompanying citations can be found in Additional file 2: Table S1.

Declarations**Ethics approval and consent to participate**

Not applicable.

Competing interests

The authors declare that they have no competing interests.

Author details

¹Department of Pulmonary Medicine, Erasmus MC, University Medical Center Rotterdam, Rotterdam, The Netherlands. ²Centre for Genomic Regulation (CRG) and Institute of Science and Technology (BIST), Barcelona, Spain. ³Universitat Pompeu Fabra (UPF), Barcelona, Spain. ⁴Aix-Marseille University, INSERM, TAGC, UMR 1090, Marseille, France. ⁵ Department of Cell Biology, Erasmus MC, University Medical Center Rotterdam, Rotterdam, The Netherlands.

Received: 9 June 2021 Accepted: 6 April 2022

Published online: 14 April 2022

References

- Zhu N, Zhang D, Wang W, Li X, Yang B, Song J, et al. A Novel Coronavirus from Patients with Pneumonia in China, 2019. *N Engl J Med.* 2020;382:727–33.
- Merad M, Martin JC. Pathological inflammation in patients with COVID-19: a key role for monocytes and macrophages. *Nat Rev Immunol.* 2020;20:355–62.
- Szabo PA, Dogra P, Gray JJ, Wells SB, Connors TJ, Weisberg SP, et al. Longitudinal profiling of respiratory and systemic immune responses reveals myeloid cell-driven lung inflammation in severe COVID-19. *Immunity.* 2021;54:797–814 e796.
- Zheng Z, Peng F, Xu B, Zhao J, Liu H, Peng J, et al. Risk factors of critical & mortal COVID-19 cases: A systematic literature review and meta-analysis. *J Inf Secur.* 2020;81:e16–25.
- Severe Covid GG, Ellinghaus D, Degenhardt F, Bujanda L, Buti M, Albillos A, et al. Genomewide Association Study of Severe Covid-19 with Respiratory Failure. *N Engl J Med.* 2020;383:1522–34.
- Pairo-Castineira E, Clohisey S, Klaric L, Bretherick AD, Rawlik K, Pasko D, et al. Genetic mechanisms of critical illness in COVID-19. *Nature.* 2021;591:92–8.
- Nakanishi T, Pigazzini S, Degenhardt F, Cordioli M, Butler-Laporte G, Maya-Miles D, et al. Age-dependent impact of the major common genetic risk factor for COVID-19 on severity and mortality. *J Clin Invest.* 2021;131(23):e152386.
- Initiative C-HG. The COVID-19 Host Genetics Initiative, a global initiative to elucidate the role of host genetic factors in susceptibility and severity of the SARS-CoV-2 virus pandemic. *Eur J Hum Genet.* 2020;28:715–8.
- Watanabe K, Taskesen E, van Bochoven A, Posthuma D. Functional mapping and annotation of genetic associations with FUMA. *Nat Commun.* 2017;1826:8.
- Stik G, Vidal E, Barrero M, Cuartero S, Vila-Casadesus M, Mendieta-Esteban J, et al. CTCF is dispensable for immune cell transdifferentiation but facilitates an acute inflammatory response. *Nat Genet.* 2020;52:655–61.
- Maurano MT, Humbert R, Rynes E, Thurman RE, Haugen E, Wang H, et al. Systematic localization of common disease-associated variation in regulatory DNA. *Science.* 2012;337:1190–5.
- Consortium EP, Moore JE, Purcaro MJ, Pratt HE, Epstein CB, Shores N, et al. Expanded encyclopaedias of DNA elements in the human and mouse genomes. *Nature.* 2020;583:699–710.
- Fernandez JM, de la Torre V, Richardson D, Royo R, Puiggros M, Moncunill V, et al. The BLUEPRINT Data Analysis Portal. *Cell Syst.* 2016;3:491–495.e495.

14. Mantovani A, Sica A, Sozzani S, Allavena P, Vecchi A, Locati M. The chemokine system in diverse forms of macrophage activation and polarization. *Trends Immunol.* 2004;25:677–86.
15. Javierre BM, Burren OS, Wilder SP, Kreuzhuber R, Hill SM, Sewitz S, et al. Lineage-Specific Genome Architecture Links Enhancers and Non-coding Disease Variants to Target Gene Promoters. *Cell.* 2016;167:1369–84 e1319.
16. Grosveld F, van Staalduinen J, Stadhouders R. Transcriptional Regulation by (Super)Enhancers: From Discovery to Mechanisms. *Annu Rev Genomics Hum Genet.* 2021;22:127–46.
17. Rapino F, Robles EF, Richter-Larrea JA, Kallin EM, Martinez-Climent JA, Graf T. C/EBP α induces highly efficient macrophage transdifferentiation of B lymphoma and leukemia cell lines and impairs their tumorigenicity. *Cell Rep.* 2013;3:1153–63.
18. Stadhouders R, Filion GJ, Graf T. Transcription factors and 3D genome conformation in cell-fate decisions. *Nature.* 2019;569:345–54.
19. Ong CT, Corces VG. CTCF: an architectural protein bridging genome topology and function. *Nat Rev Genet.* 2014;15:234–46.
20. Schioppa T, Sozio F, Barbazza I, Scutera S, Bosisio D, Sozzani S, et al. Molecular Basis for CCRL2 Regulation of Leukocyte Migration. *Front Cell Dev Biol.* 2020;8:615031.
21. Boyle AP, Hong EL, Hariharan M, Cheng Y, Schaub MA, Kasowski M, et al. Annotation of functional variation in personal genomes using RegulomeDB. *Genome Res.* 2012;22:1790–7.
22. Kircher M, Witten DM, Jain P, O’Roak BJ, Cooper GM, Shendure J. A general framework for estimating the relative pathogenicity of human genetic variants. *Nat Genet.* 2014;46:310–5.
23. Molawi K, Sieweke MH. Transcriptional control of macrophage identity, self-renewal, and function. *Adv Immunol.* 2013;120:269–300.
24. Mancino A, Termanini A, Barozzi I, Ghisletti S, Ostuni R, Prosperini E, et al. A dual cis-regulatory code links IRF8 to constitutive and inducible gene expression in macrophages. *Genes Dev.* 2015;29:394–408.
25. Toney LM, Cattoretti G, Graf JA, Merghoub T, Pandolfi PP, Dalla-Favera R, et al. BCL-6 regulates chemokine gene transcription in macrophages. *Nat Immunol.* 2000;1:214–20.
26. Chua RL, Lukassen S, Trump S, Hennig BP, Wendisch D, Pott F, et al. COVID-19 severity correlates with airway epithelium-immune cell interactions identified by single-cell analysis. *Nat Biotechnol.* 2020;38:970–9.
27. Trump S, Lukassen S, Anker MS, Chua RL, Liebig J, Thürmann L, et al. Hypertension delays viral clearance and exacerbates airway hyperinflammation in patients with COVID-19. *Nat Biotechnol.* 2021;39(6):705–16.
28. Lucas C, Wong P, Klein J, Castro TBR, Silva J, Sundaram M, et al. Longitudinal analyses reveal immunological misfiring in severe COVID-19. *Nature.* 2020;584:463–9.
29. Downes DJ, Cross AR, Hua P, Roberts N, Schwessinger R, Cutler AJ, et al. Identification of LZTF1 as a candidate effector gene at a COVID-19 risk locus. *Nat Genet.* 2021;53:1606–15.
30. Yao Y, Ye F, Li K, Xu P, Tan W, Feng Q, et al. Genome and epigenome editing identify CCR9 and SLC6A20 as target genes at the 3p21.31 locus associated with severe COVID-19. *Signal Transduct Target Ther.* 2021;6(1):85.
31. Kasela S, Daniloski Z, Bollepalli S, Jordan TX, tenOever BR, Sanjana NE, et al. Integrative approach identifies SLC6A20 and CXCR6 as putative causal genes for the COVID-19 GWAS signal in the 3p21.31 locus. *Genome Biol.* 2021;22(1):242.
32. Quinlan AR, Hall IM. BEDTools: a flexible suite of utilities for comparing genomic features. *Bioinformatics.* 2010;26:841–2.
33. Schmiedel BJ, Singh D, Madrigal A, Valdovino-Gonzalez AG, White BM, Zapardiel-Gonzalo J, et al. Impact of Genetic Polymorphisms on Human Immune Cell Gene Expression. *Cell.* 2018;175:1701–15 e1716.
34. Kim-Hellmuth S, Aguet F, Oliva M, Munoz-Aguirre M, Kasela S, Wucher V, et al. Cell type-specific genetic regulation of gene expression across human tissues. *Science.* 2020;369(6509):eaaz8528.
35. Wu C, Jin X, Tsueng G, Afrasiabi C, Su AI. BioGPS: building your own mash-up of gene annotations and expression profiles. *Nucleic Acids Res.* 2016;44:D313–6.
36. Choi J, Baldwin TM, Wong M, Bolden JE, Fairfax KA, Lucas EC, et al. Haemopedia RNA-seq: a database of gene expression during haematopoiesis in mice and humans. *Nucleic Acids Res.* 2019;47:D780–5.
37. Monaco G, Lee B, Xu W, Mustafah S, Hwang YY, Carre C, et al. RNA-Seq Signatures Normalized by mRNA Abundance Allow Absolute Deconvolution of Human Immune Cell Types. *Cell Rep.* 2019;26:1627–40 e1627.
38. Heinz S, Benner C, Spann N, Bertolino E, Lin YC, Laslo P, et al. Simple combinations of lineage-determining transcription factors prime cis-regulatory elements required for macrophage and B cell identities. *Mol Cell.* 2010;38:576–89.
39. Alasoo K, Rodrigues J, Mukhopadhyay S, Knights AJ, Mann AL, Kundu K, et al. Shared genetic effects on chromatin and gene expression indicate a role for enhancer priming in immune response. *Nat Genet.* 2018;50:424–31.
40. Quach H, Rotival M, Pothlichet J, Loh YE, Dannemann M, Zidane N, et al. Genetic Adaptation and Neandertal Admixture Shaped the Immune System of Human Populations. *Cell.* 2016;167:643–56 e617.
41. Fairfax BP, Humburg P, Makino S, Naranbhai V, Wong D, Lau E, et al. Innate immune activity conditions the effect of regulatory variants upon monocyte gene expression. *Science.* 2014;343:1246949.

Publisher’s Note

Springer Nature remains neutral with regard to jurisdictional claims in published maps and institutional affiliations.